Scilight

Advanced Antibacterial Materials

https://www.sciltp.com/journals/aam

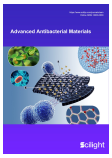

Article

Cu-Bearing Antibacterial Stainless Steel Potentiates Antibiotic Sensitivity to Combat *Methicillin-resistant Staphylococcus aureus*

Xinrui Zhang [1], Yingping Wang [2], Chunguang Yang [1,*] and Ke Yang [1,3,*]

[1] Institute of Metal Research, Chinese Academy of Sciences, Shenyang 110016, China
[2] Shandong Visee Medical Devices Co., Ltd., Weihai 264200, China
[3] Liaoning Provincial Key Laboratory of Neurointerventional Therapy and Biomaterials Research and Development, Shenyang 110016, China
* Correspondence: cgyang@imr.ac.cn (C.Y.); kyang@imr.ac.cn (K.Y.)

How To Cite: Zhang, X.; Wang, Y.; Yang, C.; et al. Cu-Bearing Antibacterial Stainless Steel Potentiates Antibiotic Sensitivity to Combat *Methicillin-resistant Staphylococcus aureus*. *Advanced Antibacterial Materials* **2025.**

Received: 6 September 2025
Revised: 15 September 2025
Accepted: 19 September 2025
Published: 30 September 2025

Abstract: Treating biofilm formation-induced implant-associated infections is challenging, and they often lead to antimicrobial resistance, which significantly contributes to human mortality worldwide. Consequently, an increase in antibiotic resistance has warranted the development of more effective strategies to combat the drug-resistant bacterial infections. Hence, this study aimed to develop an antibacterial metal implant material (Cu-bearing 316L stainless steel) as a quorum-sensing inhibitor (QSI) for reversing drug resistance in resistant bacteria. Notably, RNA sequencing results revealed that 316L-Cu SS could interfere with the formation of multidrug resistance barriers of *Methicillin-resistant Staphylococcus aureus* (MRSA), including biofilm development and metabolism, by inhibiting quorum-sensing signals. Furthermore, the resistance of MRSA to ciprofloxacin (CIP) was reversed, with up to a 67% decline in minimum bactericidal concentration. Subsequently, a QSI–CIP combination strategy was developed for synergistic action against MRSA, which achieved almost complete elimination of MRSA at low antibiotic dosage. Overall, the findings of this study present the novel antibacterial implant material as a lead QSI, highlighting the potential of adjunctive pathoblocker-mediated therapy against infections and providing a long-term activity to address the intractable challenge of drug-resistant bacteria with enhanced sustainability.

Keywords: drug-resistant bacterial; antibiotic; biofilm; Cu-bearing antibacterial stainless steel; quorum sensing

1. Introduction

In 2022, the Agency France Presse reported drug-resistant bacteria, particularly *Staphylococcus aureus*, as the leading cause of bacterial-related deaths across 135 countries. Notably, the implant-associated infections caused by drug-resistant bacteria show a mainstream trend owing to the reliance on antibiotics during therapies. Reportedly, patients infected with drug-resistant bacteria exhibit a higher mortality rate of more than 64% compared to those infected with non-resistant bacteria [1,2], presenting pathogen resistance alleviation as a major challenge in global public health. Increasing the dose or antibiotic diversity only offers a stopgap strategy, leading to a vicious cycle of drug resistance. For instance, *Methicillin-resistant Staphylococcus aureus* (MRSA) presents with the highest incidence in hospitals at an alarming rate owing to its high pathogenicity and multiple drug resistance, marking it as the main causative pathogen in the cases of osteomyelitis [3,4]. There are nearly no effective drugs that can treat MRSA in clinical settings; for example, MRSA exhibits more than 95% resistance against ciprofloxacin, a fluoroquinolone antibiotic [5,6]. These challenges have led to the delay of infection

recurrence being a common therapy endpoint rather than its eradication, highlighting the regular failure of antibiotic treatment [7,8].

To address the challenge of antibiotic resistance, studies have focused on developing antibiotic-free strategies. Biofilms are formed by the agglomeration of extracellular polymeric substances (EPS) and construct a three-dimensional mushroom-like structure to block the drug penetration, thereby leading to infection occurrence [9–11]. Reportedly, such biofilms can result in more than 10–1000 times increase in the antibiotic dosage compared with that required to eliminate the planktonic counterparts [12]. Therefore, preventing biofilm formation presents an important approach in reducing the tolerance of bacteria toward antibiotic treatment [13]. One of such approaches is the development of implants with antibacterial function to inhibit adherence of bacteria on their surface [14–16]. For example, a Cu-containing titanium alloy (Ti6Al4V-Cu) has been reported to alleviate MRSA-induced implant-associated infection based on its contact-killing antibacterial activity [17,18]. However, despite the efficacy of such antibacterial implants in infection prevention, their bactericidal performance may degrade and even disappear following the coating of the implant's surface by organic matter, which may further contribute to the persistence of infections [19,20]. These studies highlight the urgent need for the development of more effective biofilm-eliminating strategies.

Quorum sensing (QS), referred to as a virulence-controlling regulatory network, is a cell-density-dependent intercellular communication system that utilizes diffusible signal molecules, and it is involved in biofilm formation and full multidrug resistance [21]. Particularly in MRSA, QS is critically implicated in the efflux pump mechanism, which is an active response of bacteria to excrete disinfectants, acting as another drug resistance barrier in addition to biofilms. The use of QS inhibitors (QSIs) offers a so-called antagonizing drug-resistance approach for targeting QS to enhance the effectiveness of antibiotics against bacteria [22]. Notably, the implants can be used as such pathoblockers, which renders them attractive for devising an adjunctive treatment. Overall, an antibacterial implant may provide a better outcome of backbone antibiosis at the same dosage, presenting great potential to address MRSA infections.

Hence, this study aimed to develop an antibacterial Cu-bearing 316L stainless steel (316L-Cu SS) implant as a QSI, along with conducting the first proof-of-concept investigation on its efficacy to reverse the drug resistance in drug-resistant pathogens. Herein, MRSA was used to build a multidrug resistance barrier based on the biofilm model on the 316L-Cu SS surface, and ciprofloxacin (CIP) was employed for synergetic treatment. The results revealed a 67% increase in CIP-sensitivity of MRSA following 316L-Cu SS treatment, providing a solid research basis to address the challenge of drug-resistant bacteria at its root cause.

2. Experimental

2.1. Materials

The Cu-bearing 316L stainless steel (316L-Cu SS) for this study was prepared in a 25 kg vacuum induction melting furnace with chemical composition (wt.%) as follows: C 0.016, Cr 18.18, Ni 14.50, Cu 4.36, Mo 3.02, N 0.14, P 0.005, Si 0.001 and Fe in balance, while a commercial medical 316L SS was used as the control. The 316L-Cu SS was solution treated at 1100 °C for 0.5 h, followed by water cooling, so that the Cu was completely dissolved in the steel matrix. Then, the 316L-Cu SS was kept at 700 °C for 6 h to conduct aging treatment, with the purpose of precipitation of fine Cu-rich phases in the steel matrix. All the samples with a size of $\Phi 10 \times 2$ m^2 were mechanically polished up to 2000 grit before experiments. At least three parallel samples in each group were used to ensure the correctness and repeatability of results. A transmission electron microscope (TEM, FEI Tecnai G2, Eindhoven, The Netherlands) was employed to observe microstructures of the samples. For sample preparation, thin foils with a diameter of 3 mm for TEM investigation were mechanically ground to a thickness of approximately 50 μm, then electro-polished by a twin-jet Struers Tenupol-3 electro-polisher (Struers, Champigny-sur-Marne, France) in a 10 vol.% $HClO_4$ ethanol electrolyte maintained at −20 °C.

2.2. Bacterial Culture

Methicillin-resistant Staphylococcus aureus (*MRSA*, ATCC 43300) was used in the study. The bacterial suspension was prepared in Luria-Bertani (LB) media with a concentration of 10^8 CFU mL^{-1} for use.

2.3. Determination of MBC

The MBC (minimum bactericidal concentration) of CIP and the synergistic effect of CIP with experimental SS were determined using the spread plate count method. Numbered sterile tubes were prepared, and the diluted 10^7 CFU mL^{-1} bacterial suspension at a total volume of 1 mL was added. Sequentially, the concentration gradients

of CIP were prepared and were added into each tube at concentrations of 25, 50, 75, 100, 125, 150, and 200 μg mL^{-1}, respectively. After the 316L-Cu SS/316L SS samples were put into the tubes and incubated at 37 °C for 24 h, the spread plate count was conducted to quantify the MBC of CIP alone, and the MBC of CIP with the SS synergy. The turbidity of the tubes was recorded to visualize the MBC and determine the half maximal inhibitory concentration (IC_{50}).

2.4. Biofilm Phenotypes Assay

2.4.1. Biomass Assay

In a 24-well plate, 316L-Cu SS or 316L SS was incubated with 1 mL of diluted 10^7 CFU mL^{-1} MRSA at 37 °C for 24 h to obtain the biofilm formation on samples. Then the bacterial suspension was discarded, and the crystal violet was employed to detect the biomass in biofilms attached to the samples.

2.4.2. Biofilm Morphology Observation

After incubating with MRSA for 24 h, the samples were rinsed with PBS and fixed with 2.5% glutaraldehyde, followed by sequential dehydration with 50%, 60%, 70%, 80%, 90%, 95% and 100% ethanol. Next, the dried samples were gold-coated to improve the electrical conductivity of biofilms, and the morphology observation of biofilms on the samples was conducted on a scanning electron microscope (SEM, Hitachi, S-3400N). In addition, a live/dead kit was used to stain the biofilms, then a fluorescent microscope and a confocal laser scanning microscope (CLSM, MTC-600, USA) were respectively applied to observe the biofilm structures. Further, multiple-dyeing, including DAPI (4′,6-diamidino-2-phenylindole), SYPRO tangerine, and Alexa 633 conjugated concanavalin A (ConA-Alexa 633), was conducted to analyze the distribution of extracellular polymeric substance (EPS) on sample surfaces [23]. The EPS was observed using a fluorescent microscope, and the ImageJ Software was used to conduct the quantitative analyses.

2.5. QS Detection

MRSA possess two sets of quorum sensing systems, including the Agr QS system specific to Gram-positive bacteria and the LuxS system universally used in inter-species. As for the *autoinducing peptides (AIPs) detection in the* Agr QS system, MRSA was cultured overnight at 37 °C in Tryptic Soy broth (TSB). And 1.0 mL suspensions were incubated with sample at 37 °C for 10 h. Then the bacterial solution was collected and centrifuged. The supernatants were extracted and filtered. AIPs were detected directly in media filtrate using high-performance liquid chromatography-triple quadrupole linear ion trap mass spectrometer (QTRAP Enabled Triple Quad 5500+).

For autoinducers-2 (AI-2) detection in the LuxS system, after the supernatants were extracted and filtered. The autoinducers-2 (AI-2) signal reporter strain *Vibrio harveyi (V. harveyi)* BB170 was applied to detect the AI-2 signal activity [24]. In detail, the *V. harveyi* BB170 grown in autoinducer bioassay (AB) medium overnight was mixed with the extracted supernatant in a volume ratio of 1:9. After incubation for 5 h at 30 °C, the luminescence values of mixtures representing the AI-2 activity were determined using a multifunctional microplate reader.

2.6. ROS Detection

The MRSA was treated as described in Section 2.4.1, and then the bacterial cells were collected. A KeyGEN ROS Detection Kit (Beyotime, China) was employed to measure levels of the intracellular reactive oxygen species (ROS).

2.7. The Tests of QS Signals Degradation

The supernatants containing AI-2 signals were prepared as described in Section 2.5. Then a sterile supernatant was added with H_2O_2 in different concentrations. After incubation for 4 h, the expression level of AI-2 was determined.

2.8. *The Tests of QS Signals Protection*

In order to confirm the oxidative stress rendered by 316L-Cu SS for the QSI, N-acetylcysteine (NAC) as the antioxidant was added to the supernatants containing AIPs signals prepared in Section 2.5. with the final concentration of 1 mM and 10 mM, respectively. Then the mixture was incubated with 316L-Cu SS for 4 h. After incubation, the expression level of AIPs was determined.

2.9. Real-Time Quantitative PCR Analysis

RT-qPCR was employed to determine the gene expression of the efflux pump. Samples were incubated with 1 mL MRSA suspension in a 24-well plate at 37 °C overnight. The total mRNA was isolated using the RNA extraction kit (TAKARA, Nagahama-shi, Japan) and converted into cDNA with the HiScript II QRT SuperMix (Vazyme). Primer sequences of the genes are shown in Table 1. CT values were normalized to housekeeping gene (*16S*) and changes in mRNA levels of target genes were determined according to the $2^{-(\Delta\Delta CT)}$ method.

Table 1. Primers used in this study.

Genes	Primer Sequence
RT-*16S*-F	GCTCGTGTCGTGAGATGTTGG
RT-*16S*-R	TTTCGCTGCCCTTTGTATTGT
RT-*NorC*-F	AATGGGTTCTAAGCGACCAA
RT-*NorC*-R	ATACCTGAAGCAACGCCAAC

2.10. Transcriptome Analysis

10^8 CFU mL^{-1} MRSA was incubated with samples at 37 °C for 24 h. Then the bacterial cells were collected and their Gene expression analysis was analyzed by Shanghai Personalbio (Shanghai, China) using an Illumina NovaSeq 6000. Differential expression analysis of each group was performed using DESeq (v1.30.0), and genes with corrected $1 < 0.05$ and $|\log_2$(fold change (FC)$| > 1$ were assigned as significantly differentially expressed genes (DEGs). Gene ontology (GO) enrichment and Kyoto encyclopedia of genes and genomes (KEGG) pathway analyses were performed on the Personalbio Cloud Platform.

2.11. Statistical Analysis

All the experimental data were expressed as mean ± standard deviation. The Graph Pad Prism 8 statistical software was applied for the statistical analysis. One-way ANOVA was applied for the within-group comparisons. Statistical significance was determined by * $p < 0.05$, ** $p < 0.01$ and *** $p < 0.001$.

3. Results and Discussion

3.1. Synergistic Effects of 316L-Cu SS and CIP against MRSA

A constant broth dilution test was performed to determine the MBC of CIP with or without the synergy of 316L-Cu SS against MRSA. Owing to the strong CIP resistance of MRSA, the MBC of CIP was found to be 150 μg/mL, and an antibacterial rate of >99% was achieved (Figure 1a,b). Notably, the same MBC was detected in the group where CIP was co-incubated with 316L SS, indicating the ineffectiveness of 316L SS on MRSA resistance. In comparison, the MBC of CIP was reduced to 50 μg/mL with the synergy of 316L-Cu SS, reducing the dosage by 67%. Additionally, the MBC tubes of the control and CIP+316L-Cu SS groups after 24 h of exposure were recorded (Figure 1c), revealing significantly higher defecation in the suspension in the CIP + 316L-Cu SS tube, which represented lower viable bacterial counts, compared with that in the control. Accordingly, the calculated half-maximal inhibitory concentration (IC_{50}) showed an obvious decline (Figure 1d), highlighting the enhanced effectiveness of CIP in the presence of 316L-Cu SS. Overall, these results indicate that CIP could achieve a complete eradication against MRSA at a low dose with a synergy of 316L-Cu SS (Figure 1e).

3.2. Retarding Biofilm Formation by 316L-Cu SS

Drug resistance generation is a defense mechanism for bacteria, with biofilm formation being the first line of bacterial defense [25,26]. Biofilms are formed with EPS and adhere to bacterial cells to form a three-dimensional structure. These structures protect bacteria in harsh environments and prevent the penetration of any antibacterial agents, thereby lowering their efficacy to obtain drug resistance [27,28]. Herein, 316L-Cu SS upregulated the drug sensitivity of MRSA; therefore, its influence on biofilm formation was examined. Compared with the 316L SS group, the biomass accumulation on 316L-Cu SS was significantly reduced, as evidenced by the lighter color of crystal violet staining (Figure 2a,b). Moreover, after 24 h of MRSA incubation, the bacteria adhered to 316L-Cu SS were sparse (Figure 2c). Compared with the mushroom-shaped mature biofilms on 316L SS, almost no three-dimensional clumps were observed on the 316L-Cu SS surface. Additionally, the bactericidal ability of the Cu-bearing SS was nearly lost owing to rapid masking of its surface by the organic matters, such as the nutritious broth that is conducive to bacterial proliferation; most bacterial cells attached to the surface were round and full.

The three-dimensional biofilm structure remodeled by live/dead fluorescence staining showed consistency with the SEM observation (Figure 2d). Notably, weak biofilms led to higher antibiotic penetration, resulting in adequate killing efficiency (Figure 2c, red arrows). Overall, these findings indicate that 316L-Cu SS effectively limits the biofilm structure development, although bacterial viability is not the main target.

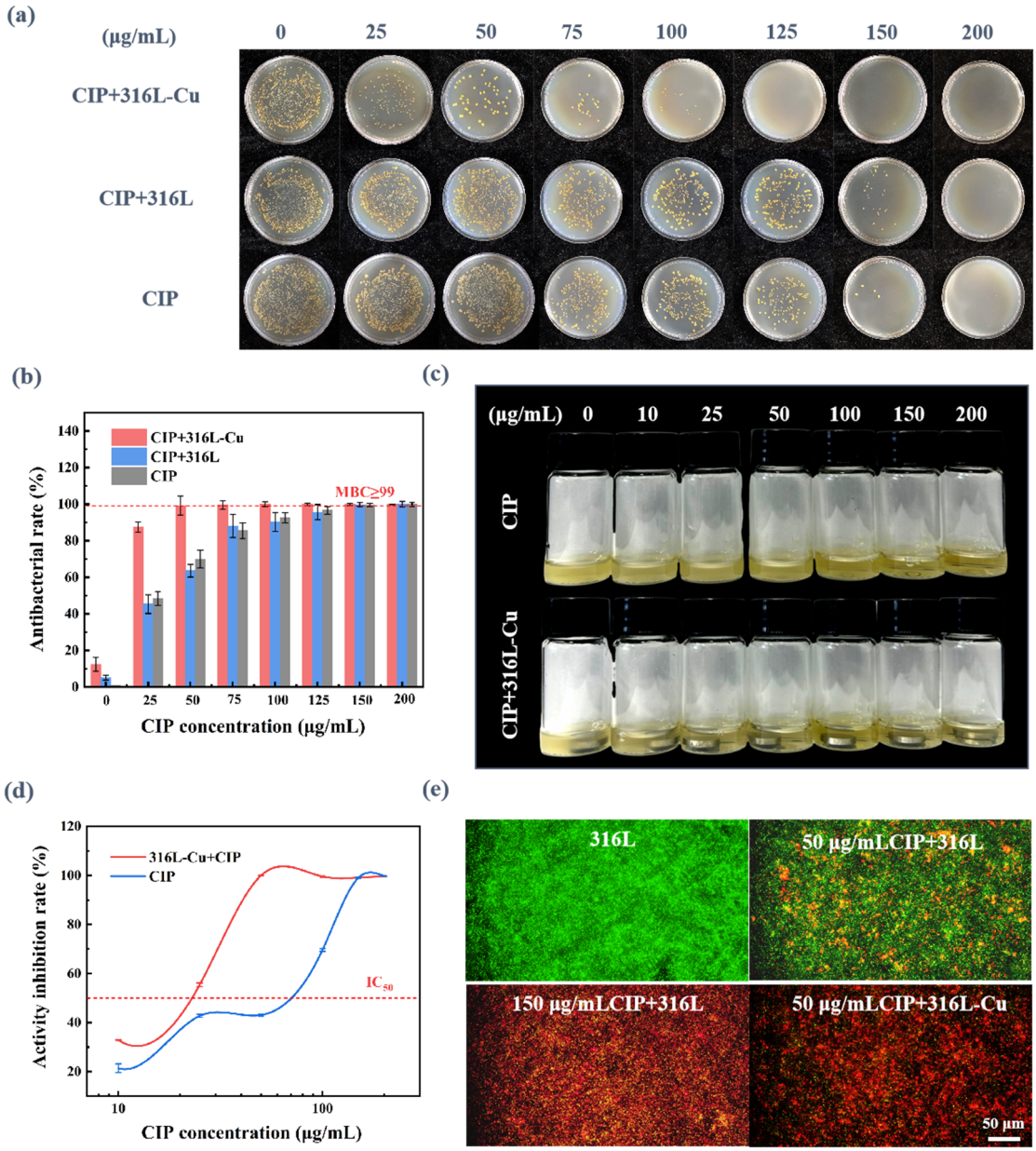

Figure 1. Antibacterial activities of CIP with and without the synergy of 316L-Cu SS, (**a**) images of MRSA colonies treated by CIP with and without different materials; (**b**) antibacterial rate of CIP with and without different materials; (**c**) turbidity images of MRSA suspension treated by CIP with and without the synergy of 316L-Cu SS; (**d**) bacterial inhibition rate of CIP with and without the synergy of 316L-Cu SS; (**e**) live/dead staining of bacterial cells attached on different materials with and without CIP treatment. Herein, the green fluorescence indicates living bacteria, and the red fluorescence indicates dead bacteria.

To explore the mechanism underlying biofilm retardation by 316L-Cu SS, the EPS section where the biofilm structure was formed under the stress of Cu-bearing SS was investigated. The triple staining technique was employed to detect the distribution of key components (cells, extracellular polysaccharides, and extracellular proteins) in the biofilms formed on different material surfaces (Figure 2e). Compared with 316L SS, 316L-Cu SS significantly inhibited the surface coverage of extracellular polysaccharides and proteins, reducing them by 16.41% and 31.57%, respectively (Figure 2f).

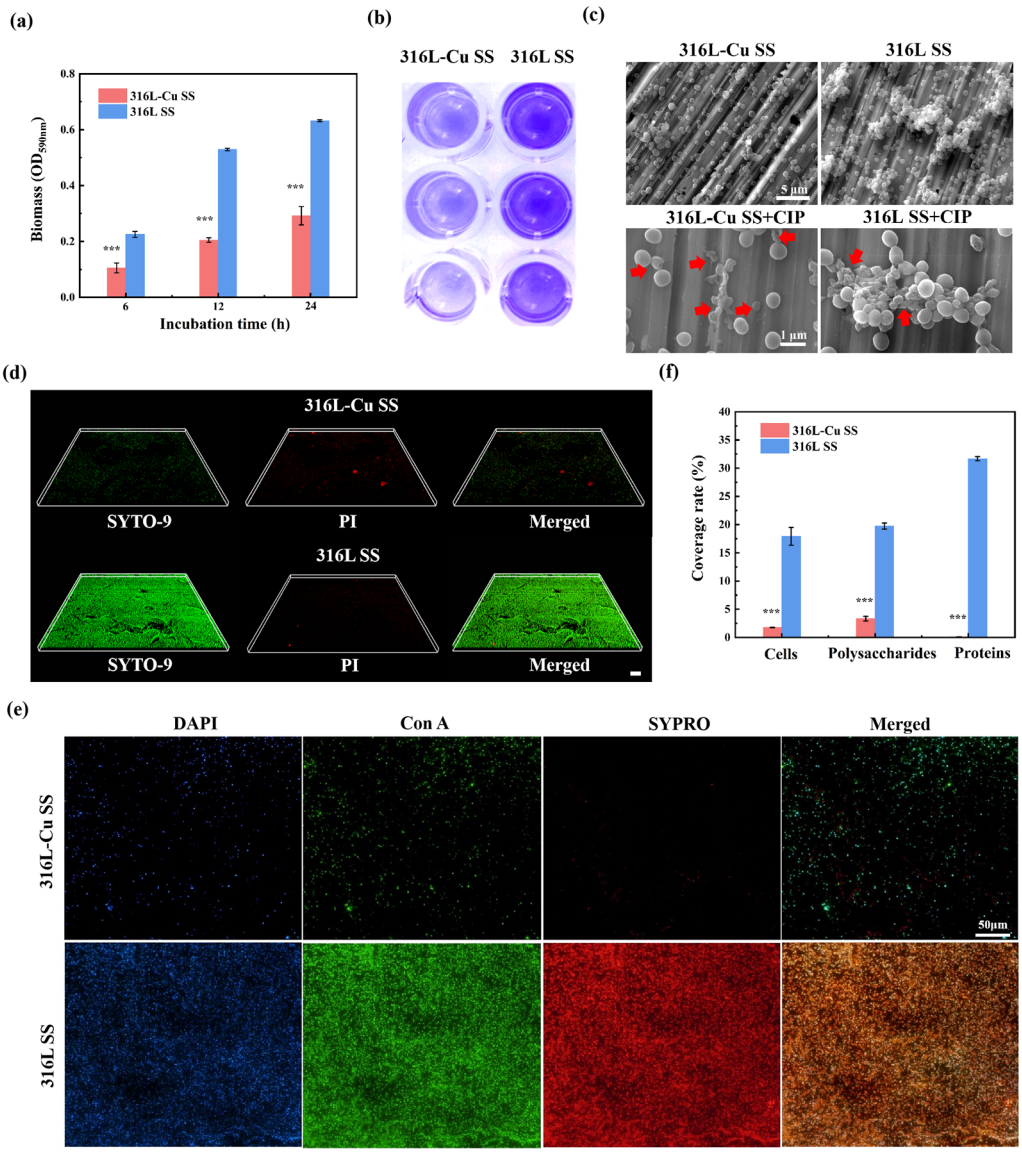

Figure 2. (**a**) Biomass on different material surfaces; (**b**) crystal violet images of collected biomass from different material surfaces; (**c**) biofilm morphologies on different materials with and without CIP treatment observed by SEM, the red arrows pointing to dead bacteria; (**d**) Live/dead staining of biofilms. Herein, the green fluorescence indicates living bacteria, and the red fluorescence indicates dead bacteria; (**e**) fluorescence images showing EPS distributions on different material surfaces. Herein, the blue fluorescence indicates bacterial cells, the green fluorescence indicates the extracellular polysaccharides, and the green fluorescence indicates the extracellular proteins; (**f**) quantitative analysis results of EPS. Asterisk indicates the significant difference between the 316L-Cu SS group and 316L SS group (*** $p < 0.001$).

3.3. Quorum Sensing Regulation by 316L-Cu SS

Bacteria use the QS system to communicate between cells, which, in turn, regulates gene expression for different functions in a population density-dependent manner [29]. Reportedly, the autoinducer-2 (AI-2)-mediated LuxS QS system is the only QS mechanism for interspecific communication that is responsible for biofilm formation, including EPS secretion and the regulation of the capsular polysaccharide of *S. aureus* [30]. Hence, the AI-2 QS signals were detected in MRSA-derived supernatants exposed to 316L-Cu SS. Notably, the signal exhibited high activity before the stationary growth (Figure 3a), which is consistent with the reported production rule of AI-2 in bacterial cells [31]. Meanwhile, AI-2 activities significantly decreased in 316L-Cu SS-exposed MRSA at different times, suggesting its QSI role for AI-2. Furthermore, as a gram-positive bacterium, MRSA is driven by the Agr QS system for virulence expression, including the overexpression of efflux pumps, which actively pump detrimental antibiotics out of bacterial cells. As shown in Figure 3b, 316L-Cu stainless steel also exhibited a QSI effect on AIP signaling molecules associated with Agr system. Consequently, the gene expression of the key efflux pump *NorA* was significantly reduced (Figure 3c).

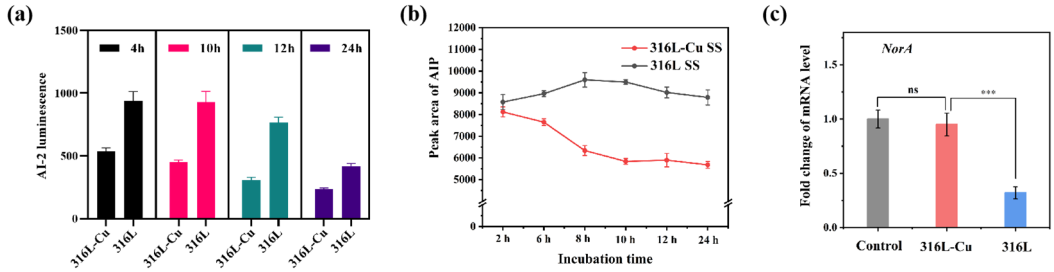

Figure 3. (**a**) AI-2 activity produced by MRSA after incubation with different materials; (**b**) AIPs activity produced by MRSA after incubation with different materials; (**c**) Expression of typical efflux pump genes *NorA* of MRSA after different treatments. Asterisk indicates the significant difference between the 316L-Cu SS group and 316L SS group (*** $p < 0.001$).

Mechanistically, QS micromolecules can be oxidized by reactive oxygen species (ROS) [32]. Following antibacterial heat treatment, large amounts of nano-scale, spheroidal, and fine Cu-rich precipitates were found to be distributed evenly in the 316L-Cu SS (Figure 4a,b). Our previous research has clarified that the formed micro-galvanic cells composed of nano Cu-rich phase and steel matrix is the driving force for Cu release, then inducing the charge transfer reaction with bacterial cells, and taking the bacterial metabolite H_2O_2 served as a precursor to induce the Fenton-type reaction and produce highly reactive ROS as follow:

$$Cu^{+} + H_2O_2 \rightarrow Cu^{2+} + OH^{-} + \cdot OH \quad (1)$$

In contrast, the Cu-bearing SS that has not undergone aging heat treatment for Cu-rich phase precipitation showcases the inability to trigger significant ROS [33]. Based on this, the 2,7-dichloro-dihydrofluorescein diacetate (DCFH-DA) dye was used to measure the related ROS generation. As expected, the expression of ROS significantly increased in MRSA treated by 316L-Cu SS with abundant copper-rich precipitation. To further detect the role of ROS in QS, H_2O_2, as a kind of exogenous ROS, was applied to evaluate the stability of separated AI-2 signal molecules under the ROS stress. A low concentration of ROS was shown to induce substantial QS inhibition (Figure 4e). Besides, gradient concentrations of *N*-acetyl-*L*-cysteine (NAC, an antioxidant reagent) were added to the 316L-Cu SS group for shielding ROS, and the intensity of AIPs gradually increased (Figure 4f). Altogether, these results suggest that 316L-Cu SS can act as QSI through inducing ROS production, resulting in structural defects of biofilm development and efflux pump, and ultimately weakening the bacterial resistance.

3.4. Transcriptome Sequence Analyses

The precise molecular mechanisms underlying 316L-Cu SS activity against MRSA were evaluated through the transcriptomics analyses of bacterial cells treated with 316L-Cu SS and 316L SS. In total, 2240 genes, with 71 of them being differentially expressed genes (DEGs) (DESeq2 at fold-change > 2 and false discovery rate-adjusted $p < 0.05$), were identified in the 316L-Cu SS group. The cluster analysis of DEGs was performed (Figure 5a), and regions in different colors represented different cluster grouping information, whereas similarly colored regions indicated the regulation of the same pathway by the corresponding genes. These results facilitated the identification of differences in the MRSA population affected by 316L-Cu SS and 316L SS. Volcano plots further visualized the differential expressions among MRSA treated with 316L-Cu SS and 316L SS. Notably, 51 genes in 316L-Cu SS-treated MRSA were upregulated, and 20 genes were downregulated compared with those in the control group (Figure 5b). Gene ontology (GO) analysis was performed to reveal the functional categories of DEGs, which revealed gene enrichment in the biological processes such as arginine biosynthesis and metabolism, along with glutamine family amino acid biosynthesis (Figure 5c). Additionally, DEGs of canonical pathways in the Kyoto encyclopedia of genes and genomes (KEGG) analysis were mapped to find the pathways that responded to 316L-Cu SS (Figure 5d).

KEGG analysis revealed that the drug-resistance-related pathways were significantly enriched, including galactose metabolism, arginine biosynthesis, QS, and ATP-binding cassette (ABC) transporter pathways. Galactose metabolism has been implicated in the antibacterial function and plays an important role in the anti-MRSA process, as it is the most important metabolism pathway for bacterial survival and a major component in cell wall polymers, glycolipids, and glycoproteins [34]. Notably, *S. aureus* can exclude antibiotics and QS signals from the cell through ABC transporters utilizing ATP hydrolysis-derived energy to obtain bacterial antibiotic resistance, which is an important reason for the drug resistance in MRSA [35,36]. Reportedly, knockout of regulatory

genes of the ABC transporters has been associated with an increase in the drug susceptibility of bacteria [37]. Furthermore, arginine deletion has been shown to lead to ROS accumulation [38].

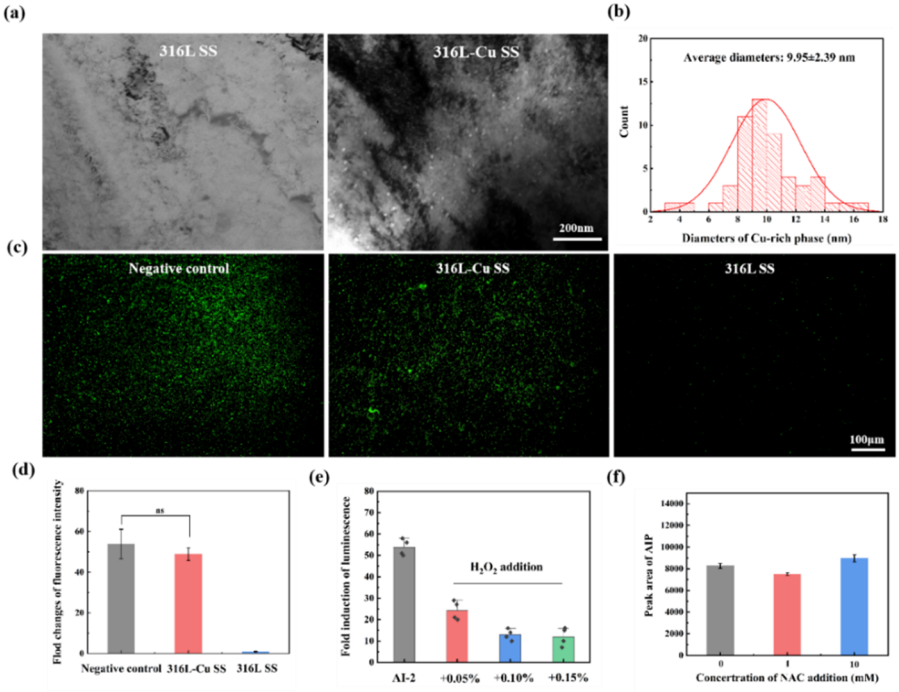

Figure 4. (**a**) TEM bright-field micrographs of 316L SS and 316L-Cu SS; (**b**) Size distribution of Cu-rich phase in 316L-Cu SS; (**c**) Fluorescence images of ROS produced by MRSA after incubation with different materials; (**d**) Quantified fluorescence intensity of ROS produced by MRSA after incubation with different materials; (**e**) Impact of H_2O_2 with different concentrations on AI-2 activity; (**f**) AIP intensities changes after supplement with NAC in 316L-Cu SS groups.

Most critically, QS that regulates biofilm formation and participates in bacterial drug resistance was significantly enriched [39], which confirmed the key role of 316L-Cu SS as QSI (Figure 5e). Altogether, these results indicate that the Cu-bearing SS induces ROS generation, thereby resulting in metabolic disorders and obstruction of resistance pathways in MRSA. Moreover, the disturbance of arginine biosynthesis further exacerbated ROS accumulation, enhancing the dismantling of resistance barriers

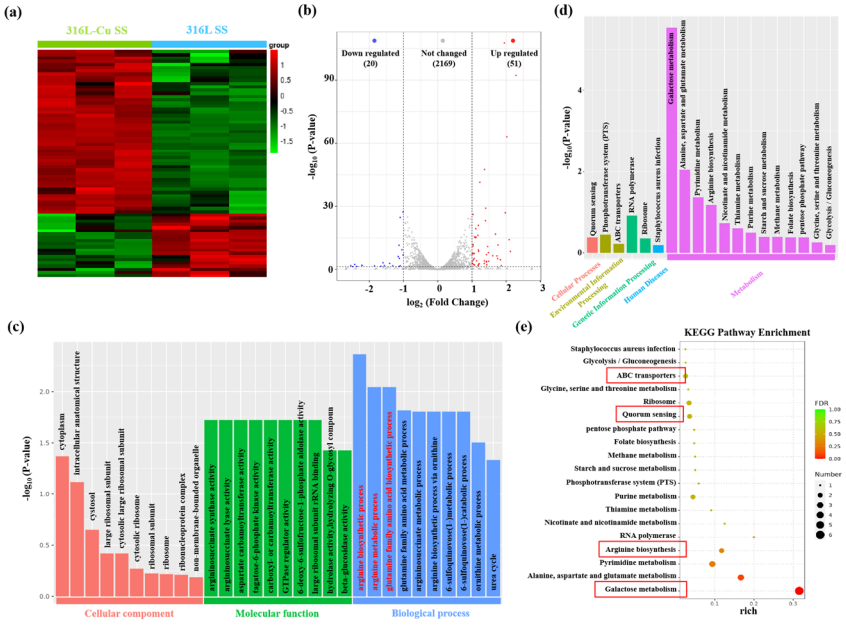

Figure 5. (**a**) Cluster analysis of DEGs; (**b**) volcano map for the distribution of DEGs; (**c**) GO enrichment analysis of DEGs; (**d**) DEGs enriched in KEGG pathway; (**e**) larger bubbles contain more DEGs.

4. Conclusions

This study reveals an innovative strategy for devising an adjunctive treatment utilizing antibacterial metal implants. Specifically, 316L-Cu SS was developed as a potential implant material to ultimately reduce the extracellular and intracellular resistance barriers of drug-resistant bacteria, namely MRSA. The proposed strategy could inhibit biofilm development, QS, and resistance pathways. This inhibition activity of 316L-Cu SS may provide a window period to promote the efficiency of antibiotics on bacteria, thereby improving the outcome of backbone antibiosis. Altogether, the findings in this study provide a novel strategy for treating the implant-associated, drug-resistant infections and address the lowering of the risk of subsequent resistance development.

Author Contributions

X.Z.: conceptualization, methodology, data curation, writing—original draft preparation; Y.W.: visualization, investigation; C.Y.: writing—reviewing and editing; K.Y.: supervision. All authors have read and agreed to the published version of the manuscript.

Funding

This work was supported by the National Natural Science Foundation of China (Grant No. 52301307 and 52171242), the Natural Science Foundation of Liaoning Province (Grant No. 2024-BABA-48), the IMR Innovation Fund (Grant No. 2022-PY18), and the Research and Development of Special Stainless Steel for Medical Use with High Strength and Corrosion Resistant (Grant No. 2024C01151).

Data Availability Statement

The data in the current study are available from the corresponding author on reasonable request.

Conflicts of Interest

The authors declare no conflict of interest.

References

1. Baker, R.E.; Mahmud, A.S.; Miller, I.F.; et al. Infectious disease in an era of global change. *Nat. Rev. Microbiol.* **2022**, *20*, 193–205.
2. Kumar, K.; Chopra, S. New drugs for *Methicillin-resistant Staphylococcus aureus*: An update. *J. Antimicrob. Chemother.* **2013**, *68*, 1465–1470.
3. Fisher, R.A.; Gollan, B.; Helaine, S. Persistent bacterial infections and persister cells. *Nat. Rev. Microbiol.* **2017**, *15*, 453–464.
4. Turner, N.A.; Sharma-Kuinkel, B.K.; Maskarinec, S.A.; et al. *Methicillin-resistant Staphylococcus aureus*: An overview of basic and clinical research. *Nat. Rev. Microbiol.* **2019**, *17*, 203–218.
5. Blair, J.M.; Webber, M.A.; Baylay, A.J. et al. Molecular mechanisms of antibiotic resistance. *Nat. Rev. Microbiol.* **2015**, *13*, 42–51.
6. Kurlenda, J.; Grinholc, M. Alternative therapies in *Staphylococcus aureus* diseases. *Acta Biochim. Pol. 2012 59*, 171–184.
7. Palser, S.; Smith, S.; Nash, E.F.; et al. Treatments for preventing recurrence of infection with *Pseudomonas aeruginosa* in people with cystic fibrosis (Protocol). *Cochrane Database Syst. Rev.* **2019**, *12*, CD012300.
8. Malhotra, S.; Hayes, D.; Wozniak, D.J. Cystic fibrosis and *Pseudomonas aeruginosa*: The host-microbe interface. *Clin. Microbiol. Rev.* **2019**, *32*, e00138-18.
9. Cos, P.; Tote, K.; Horemans, T. Biofilms: An extra hurdle for effective antimicrobial therapy. *Curr. Pharm. Des.* **2010**, *16*, 2279–2295.
10. Costerton, W.; Veeh, R.; Shirtliff, M.; et al. The application of biofilm science to the study and control of chronic bacterial infections. *J. Clin. Investig.* **2003**, *112*, 1466–1477.
11. Petit, T.J.P.; Lebreton, A. Adaptations of intracellular bacteria to vacuolar or cytosolic niches. *Trends Microbiol.* **2022**, *30*, 736–748.
12. Rumbaugh, K.P.; Sauer, K. Biofilm dispersion. *Nat. Rev. Microbiol.* **2020**, *18*, 571–586.
13. Schütz, C.; Empting, M.; Beilstein, J. Targeting the *Pseudomonas* quinolone signal quorum sensing system for the discovery of novel anti-infective pathoblockers. *Beilstein J. Org. Chem.* **2018**, *14*, 2627–2645.
14. Guan, W.; Tan, L.; Liu, X.; et al. Ultrasonic interfacial engineering of red phosphorous-metal for eradicating mrsa infection effectively. *Adv. Mater.* **2021**, *33*, 2006047.

15. Chai, H.W.; Guo, L.; Wang, X.T.; et al. Antibacterial effect of 317L stainless steel contained copper in prevention of implant-related infection in vitro and in vivo. *J. Mater. Sci. Mater. Med.* **2011**, *22*, 2525–2535.
16. Zhao, J.; Cao, Z.Q.; Ren, L.; et al. A novel ureteral stent material with antibacterial and reducing encrustation properties. *Mater. Sci. Eng. C* **2016**, *68*, 221–228.
17. Zhuang, Y.F.; Ren, L.; Zhang, S.Y.; et al. Antibacterial effect of a copper-containing titanium alloy against implant-associated infection induced by *methicillin-resistant Staphylococcus aureus*. *Acta Biomater.* **2021**, *119*, 472–484.
18. Zhang, X.R.; Yang, C.G.; Xi, T.; et al. Cu-bearing stainless steel affects its contact-killing efficiency by mediating the interfacial interaction with bacteria. *ACS Appl. Mater. Interfaces* **2021**, *13*, 2303–2315.
19. Natan, M.; Edin, F.; Perkas, N.; et al. Two are better than one: Combining ZnO and MgF_2 nanoparticles reduces *Streptococcus pneumoniae* and *Staphylococcus aureus* biofilm formation on cochlear implants. *Adv. Funct. Mater.* **2016**, *26*, 2473–2481.
20. Xing, J.; Qi, S.; Wang, Z.; et al. Antimicrobial peptide functionalized conductive nanowire array electrode as a promising candidate for bacterial environment application. *Adv. Funct. Mater.* **2019**, *29*, 1806353.1–1806353.9.
21. Wagner, S.; Sommer, R.; Hinsberger, S.; et al. Novel strategies for the treatment of pseudomonas aeruginosa infections. *J. Med. Chem.* **2016**, *59*, 5929–5969.
22. Christian, Schütz.; Ho, D.K.; Hamed, M.M.; et al. A new PqsR inverse agonist potentiates tobramycin efficacy to eradicate *Pseudomonas aeruginosa* biofilms. *Adv. Sci.* **2021**, *8*, 2004369.
23. Liu, R.; Tang, Y.L.; Zeng, L.L.; et al. In vitro and in vivo studies of anti-bacterial copper-bearing titanium alloy for dental application. *Dent. Mater.* **2018**, *34*, 1112–1126.
24. Xiao, X.; Zhu, W.; Liu, Q.; et al. Impairment of biofilm formation by TiO_2 photocatalysis through quorum quenching. *Environ. Sci. Technol.* **2016**, *50*, 11895–11902.
25. Truong-Bolduc, Q.C.; Strahilevitz, J.; Hooper, D.C. NorC, a new efflux pump regulated by MgrA of *Staphylococcus aures*. *Antimicrob Agents Chemother* **2006**, *50*, 1104–1107.
26. Høiby, N.; Bjarnsholt, T.; Givskov, M.; et al. Antibiotic resistance of bacterial biofilms. *Int. J. Antimicrob. Agents* **2010**, *35*, 322–332.
27. Prakash, B.; Veeregowda, B.; Krishnappa, G. Biofilms: A survival strategy of bacteria. *Curr. Sci.* **2003**, *85*, 1299–1307.
28. Costerton, J.W.; Lewandowski, Z.; Caldwell, D.E.; et al. Microbial biofilms. *Annu. Rev. Microbiol.* **1995**, *49*, 711–745.
29. Xavier, K.; Bassler, B. Interference with AI-2-mediated bacterial cell-cell communication. *Nature* **2005**, *437*, 750.
30. Zhao, L.; Xue, T.; Shang, F.; et al. *Staphylococcus aureus* AI-2 quorum sensing associates with the KdpDE two-component system to regulate capsular polysaccharide synthesis and virulence. *Infect. Immun.* **2010**, *78*, 3506–3515.
31. Li, M.; Villaruz, A.E.; Vadyvaloo, V.; et al. AI-2-dependent gene regulation in staphylococcus epidermidis. *BMC Microbiol.* **2008**, *8*, 4.
32. Zhang, X.L.; Lee, K.; Yu, H.R.; et al. Photolytic quorum quenching: A new anti-biofouling strategy for membrane bioreactors. *Chem. Eng. J.* **2019**, *378*, 12223–12232.
33. Zhang, X.R.; Yang, C.G.; Yang, K. Contact killing of Cu-bearing stainless steel based on charge transfer caused by the microdomain potential difference. *ACS Appl. Mater. Interfaces* **2020**, *12*, 361–372.
34. Crowe, M.; O'Sullivan, M.; Cassetti, O.; et al. Estimation and consumption pattern of free sugar intake in 3-year-old Irish preschool children. *Eur. J. Nutr.* **2020**, *59*, 2065–2074.
35. Orelle, C.; Mathieu, K.; Jault, J.M. Multidrug ABC transporters in bacteria. *Res. Microbiol.* **2019**, *170*, 381–391.
36. Barbosa, T.M.; Levy, S.B. The impact of antibiotic use on resistance development and persistence. *Drug Resist. Updates* **2000**, *3*, 303–311.
37. Huda, N.; Lee, E.W.; Chen, J.; et al. Molecular cloning and characterization of an ABC multidrug efflux pump, VcaM, in Non-O1 *Vibrio cholerae*. *Antimicrob. Agents Chemother.* **2003**, *47*, 2413–2417.
38. Tiwari, S.; Van Tonder, A.J.; Vilchèze, C.; et al. Arginine-deprivation induced oxidative damage sterilizes mycobacterium tuberculosis. *Proc. Natl. Acad. Sci. USA* **2018**, *115*, 9779–9784.
39. Suga, H.; Smith, K.M. Molecular mechanisms of bacterial quorum sensing as a new drug target. *Curr. Opin. Chem. Biol.* **2003**, *7*, 586–591.